

with

$$u' \cong E c^2 p p_y \sin \theta \cos \theta / D', \quad v' \cong [(E \sin^2 \theta - E_0 \cos^2 \theta) c^2 p p_x + i E_0 \cos^2 \theta c^2 p p_y] / D',$$

$$D' = (E + E_0)(E^2 - c^2 p^2 \cos^2 \theta).$$

In the expressions for u' and v' , only terms linear in p_x and p_y have been retained. The transformation matrix RT has eigenvalues of the form $\exp(\pm i\varphi')$. If the dependence of φ' on p_x is made insignificant by choosing a beam well collimated in the x direction, or by choosing $\tan^2 \theta \cong E_0/E$, then φ' is approximately linear in $|p_y|$ and for m similar reflections the shifts normal to the plane of incidence will be

$$\Delta y = \mp m \hbar (\partial \varphi' / \partial p_y) = \mp m \hbar c^2 p \cos \theta (E + E_0)^{-1} (E^2 - c^2 p^2 \cos^2 \theta)^{-1/2}.$$

The eigenvectors in this case correspond to spin polarizations in the plane of incidence. These shifts normal to the plane of incidence would be much harder to observe experimentally than those in the plane of incidence since it would be necessary to rotate the spin very precisely between reflections.

It is to be expected that other particles with spin would lead to similar shifts on reflection. Unfortunately, the characteristic sizes of these shifts are of the order of the Compton wavelengths of the particles, and thus it will be very difficult to observe these effects experimentally.

¹N. Ashby and S. C. Miller, Jr., to be published.

²F. Goos and M. Hänchen, *Ann. Phys. (Paris)* **1**, 333 (1947).

³C. Imbert, *Phys. Rev. D* **5**, 787 (1972).

⁴O. Costa de Beauregard and C. Imbert, *Phys. Rev. Lett.* **28**, 1211 (1972).

⁵*Handbook of Mathematical Functions*, edited by M. Abramowitz and I. A. Stegun (U. S. GPO, Washington, D. C., 1964), p. 504.

Inclusive Pion Distributions in Electroproduction*

E. Lazarus,† D. Andrews, K. Berkelman, G. Brown, D. G. Cassel, W. R. Francis, D. L. Hartill, J. Hartmann, R. M. Littauer, R. L. Loveless, R. C. Rohlfs, and D. H. White
Laboratory of Nuclear Studies, Cornell University, Ithaca, New York 14850

and

A. J. Sadoff

Physics Department, Ithaca College, Ithaca, New York 14850

(Received 20 July 1972)

Measurements are reported for the process $e + p \rightarrow e + \pi^+ + \text{anything}$. Partial multiplicities and average transverse momenta show no significant dependence on Q^2 .

The recent experimental data¹ on inelastic electron scattering at high energies have stimulated much theoretical speculation.² In the hope of learning more than can be obtained from electron data alone, we have measured the yield of positive pions in coincidence with the scattered electrons.

The external electron beam of the Cornell synchrotron struck a 2.7-cm liquid hydrogen target and was monitored in a Faraday cup. Inelastically scattered electrons passed through a spectrometer consisting of two quadrupoles and two bending magnets and were detected in eight pro-

portional wire chamber planes, two scintillators, a Freon gas Cherenkov counter, and a lead-acetate shower Cherenkov counter. The spectrometer had an aperture of 0.5 msr and an rms momentum resolution of 0.3%. It was placed at 6.6° and 9.0° laboratory scattering angles for the measurements described here.

Positive pions produced in the laboratory angle range between about 45° and 80° and at elevation angles within $\pm 10^\circ$ passed through the aperture of a bending magnet, two wide-gap optical spark chambers, and a double bank of trigger scintillators. All momenta above 150 MeV/c were de-

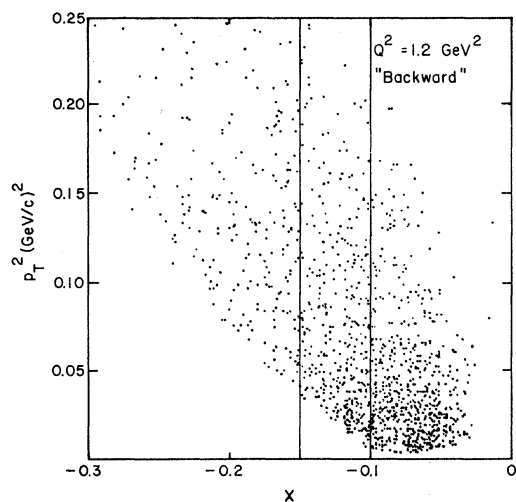


FIG. 1. Sample distribution of electroproduced π^+ in p_T^2 versus x , in the γ (virtual) + p center-of-mass frame. The longitudinal axis is the virtual-photon direction. The vertical band shows one of the x regions over which the data are averaged in obtaining Figs. 2 and 3.

tectable. Pions were identified by comparing the measured time of flight (1 nsec rms resolution) with that calculated for the observed momentum and path length (typically 2.5 m). Contamination of K^+ and p was less than 5% for momenta below 750 MeV/c.

The electron four-momentum transfer Q^2 and the total center-of-mass energy W of the hadron final state are fixed by the incident and scattered electron energies and the scattering angle. These were chosen to correspond to $Q^2 = 0.3, 0.6,$ and 1.2 GeV^2 with W centered on 3.0 GeV in each case. For each of the three Q^2 values, measurements were made with two positions of the pion spark chambers, "forward" and "backward." Data were corrected for detection efficiencies, geometric acceptance, pion decays, random coincidences, and target-wall background. No radiative correction has been made. The radiative effect on Q^2 and W is insignificant compared with the experimental apertures, typically $\pm 10\%$ in each; it mainly affects the overall cross-section normalization, but by less than 10%.

For each event we compute p_L and p_T in the hadron final-state center-of-mass frame, with respect to the momentum-transfer (virtual photon) direction. Figure 1 shows the distribution of events in $x = p_L/p_{\text{max}}$ versus p_T^2 for one of the six running conditions. The corresponding plots for the other five conditions look very similar, except that the detected region (defined by the pion chamber location) shifts to somewhat more

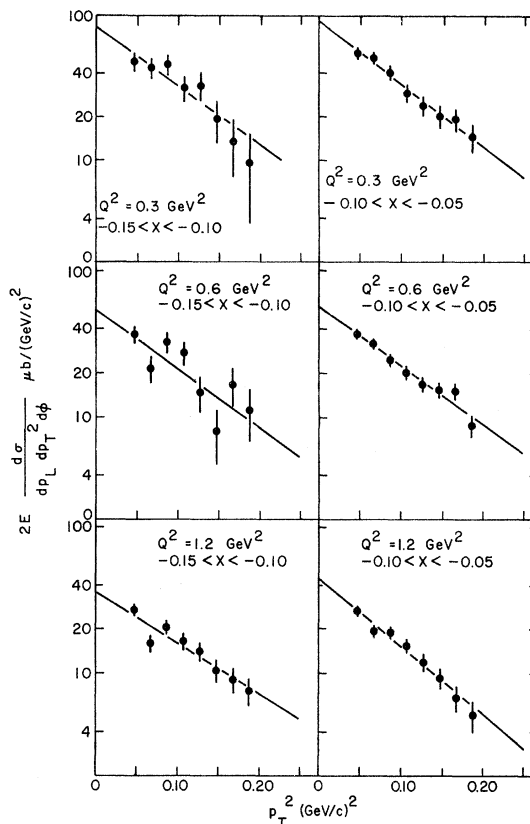


FIG. 2. Transverse momentum distributions for the three Q^2 values and two different ranges in x . W is fixed at 3 GeV.

positive x in the three "forward" measurements. The most striking feature of the data in each case is the rapid decrease in yield with increasing transverse momentum p_T .

This is seen more clearly in Fig. 2 where we plot the measured invariant cross sections³ $2E d^2\sigma/dp_L dp_T^2 d\phi$ for the process γ (virtual) + $p \rightarrow \pi^+ + \text{anything}$,⁴ versus the square of the transverse momentum,⁵ averaged over a band in x such as that indicated in Fig. 1. In each case the data are fitted very well by the form $A \exp(-Bp_T^2)$; the best-fit intercepts and slopes are given in Table I. Within statistical error (about 10%) all the data are consistent with $B = 9.5 \text{ GeV}^{-2}$. This corresponds to an rms transverse momentum of about 230 MeV/c for $Q^2 = 0.3$ to 1.2 GeV^2 , $W = 3.0 \text{ GeV}$, and small negative x . It has been suggested⁶ that the photon-proton interaction may become more pointlike as the virtual photon becomes more spacelike, resulting in an increase in the transverse momenta of the secondary products. No such increase is seen in the present data, although it is still possible that such an effect might be associated only with the virtual-photon

TABLE I. Experimental results. $\Delta\sigma$ is the cross section for $\gamma(\text{virtual}) + p \rightarrow \pi^+ + \text{anything}$, integrated over the specified x range. σ is the corresponding total cross section for $\gamma(\text{virtual}) + p \rightarrow \text{anything}$, interpolated from data of Ref. 1. See text for other definitions.

Q^2 (GeV^2)	0.3	0.3	0.6	0.6	1.2	1.2
geometry	back	fwd	back	fwd	back	fwd
$E_{e,\text{inc}}$ (GeV)	7.5	7.5	9.5	9.5	10.0	10.0
$E_{e,\text{scat}}$ (GeV)	3.0	3.1	4.9	4.9	5.0	5.0
θ_e (degrees)	6.6	6.7	6.6	6.7	9.0	9.0
A ($\mu\text{b}/\text{GeV}^2$)	85 ± 14	90 ± 10	54 ± 10	56 ± 6	36 ± 4	44 ± 2
B (GeV^{-2})	8.4 ± 1.8	9.9 ± 1.1	9.4 ± 1.9	9.3 ± 0.9	8.0 ± 1.1	10.8 ± 1.0
x_{min}	-0.15	-0.10	-0.15	-0.10	-0.15	-0.10
x_{max}	-0.10	-0.05	-0.10	-0.05	-0.10	-0.05
$\Delta\sigma$ (μb)	5.2 ± 0.5	5.6 ± 0.3	3.8 ± 0.3	3.8 ± 0.2	2.5 ± 0.1	2.7 ± 0.1
σ (μb)	77.3	76.4	52.7	52.0	33.4	33.0

fragments in the forward hemisphere ($x > 0$).

Since the present data were obtained at a fixed value of $W [=s^{1/2}$ for the process $\gamma(\text{virtual}) + p$], it is not possible to check for Feynman scaling.⁷ To look at the Q^2 dependence we integrate the observed $d\sigma/dx dp_T^2 d\varphi$ over the appropriate x band, over all p_T^2 (assuming the best fit), and over φ

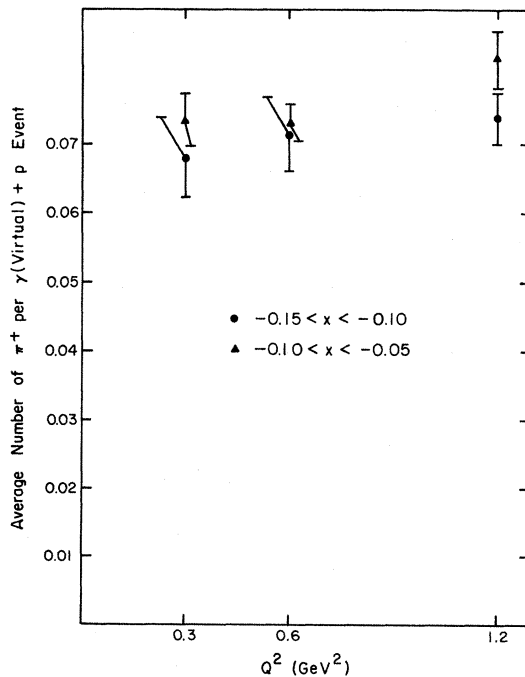


FIG. 3. The number per $\gamma(\text{virtual}) + p$ event of π^+ 's produced into the specified x range, as a function of Q^2 . This given by the ratio $\Delta\sigma/\sigma$ (Table I).

(assuming no φ variation), then divide by the total $\gamma(\text{virtual}) + p$ cross section for that Q^2 and W , obtained from the electron single-arm scattering data.¹ The result represents the average multiplicity of positive pions produced in the specified x range. This is shown in Fig. 3. It is interesting to note that although the yield shows the usual decrease with increasing $|x|$, there is little or no dependence⁸ on Q^2 . Apparently the increase in multiplicity suggested by some models⁹ is not taking place at small negative x .

As a by-product of this experiment, a limited amount of π^- data is available¹⁰ centered on $x = -0.3$. Within the errors the p_T and Q^2 dependences are the same as in the π^+ case.

*Work supported by the National Science Foundation.

†Present address: Brookhaven National Laboratory, Upton, New York 11473.

¹G. Miller *et al.*, Phys. Rev. D **5**, 528 (1972).

²For several recent reviews of the abundant theoretical literature, see *Proceedings of the Fifth International Symposium on Electron and Photon Interactions at High Energies, 1971*, edited by N. B. Mistry (Cornell Univ. Press, Ithaca, New York, 1972).

³ E is the pion energy in the center of mass of the reaction $\gamma(\text{virtual}) + p$; φ is the azimuth of the pion about the virtual-photon direction. The factor 2 arises from the fact that the appropriate differential in transverse momentum is $\frac{1}{2} dp_T^2 = p_T dp_T$.

⁴The usual virtual-photon flux factor Γ has been divided out of the measured electroproduction differential cross section. For the definition of Γ , see, for example, Ref. 2, page 264.

⁵Although the pion detection system is sensitive beyond $p_T=0.45$ GeV, such events are not included in the present analysis, since the separation between pions and other particles is less certain at the high momenta.

⁶H. Cheng and T. T. Wu, Phys. Rev. **183**, 1324 (1969); R. W. Griffith, Phys. Rev. **188**, 2112 (1969); J. D. Bjorken, J. B. Kogut, and D. E. Soper, Phys. Rev. D **3**, 1382 (1971).

⁷R. P. Feynman, Phys. Rev. Lett. **23**, 1415 (1969).

⁸A preliminary analysis of the present data showed a possible increase with Q^2 (see Ref. 2, p. 276). This was based on a rather crude treatment of the geometric acceptance and is superseded by the analysis reported here.

⁹See for example T. T. Chou and C. N. Yang, Phys. Rev. D **4**, 2005 (1971).

¹⁰We are indebted to T. Killian for the analysis of the negative pion data.

Measurement of the Inclusive Electroproduction of Hadrons*

J. T. Dakin, G. J. Feldman, W. L. Lakin,† F. Martin, M. L. Perl, E. W. Petraske,‡ and W. T. Toner§
Stanford Linear Accelerator Center, Stanford University, Stanford, California 94305
 (Received 31 July 1972)

The electroproduction of hadrons was studied with a wide-aperture spectrometer. Inclusive data are presented for the electron-scattering region $-0.5 > q^2 > -2.5$ (GeV/c)², $4 < \nu < 14$ GeV. Distributions of the electroproduced hadrons in the three inclusive variables φ , p_{\perp}^2 , and x are studied in the region $x > 0$. A striking difference from photoproduction is observed in the excess of positive over negative hadrons at high x and high q^2 .

With the recent work in deep inelastic electron-nucleon scattering and its subsequent theoretical interpretations, there has been increasing interest in the hadronic final states produced in such interactions.¹ Here we report some preliminary results on the inclusive electroproduction of hadrons.

In this experiment, we detected in coincidence an electron scattered from a hydrogen target and one or more electroproduced hadrons. Taking each combination of a scattered electron and an electroproduced hadron as an independent inclusive event, the cross section is a function of six variables. Three of them are determined by the electron system: E , the incident electron energy in the laboratory (fixed at 19.5 GeV for all of our data); q^2 , the invariant momentum transfer squared to the scattered electron; and ν , the electron energy loss in the laboratory. The remaining three, which concern the detected hadron, are calculated relative to the direction of the electron three-momentum transfer: x , the ratio of the longitudinal momentum in the virtual-photon production center-of-mass system to the maximum possible; p_{\perp}^2 , the transverse momentum squared; and φ , the hadron azimuthal angle.

Virtual photoproduction cross sections can be derived from experimental cross sections by

$$\frac{d\sigma}{dq^2 d\nu d^3p} = \Gamma(E, q^2, \nu) \frac{d\sigma(q^2, \nu)}{d^3p}, \quad (1)$$

where the function Γ contains the electrodynamic factors describing the electron-photon vertex.

We will report here ratios of differential virtual-photon cross sections to the total virtual-photon cross section. These ratios are derived directly from our data since we had no requirement for a hadron in our trigger.

The differential cross sections will be given in a Lorentz-invariant form:

$$E \frac{d\sigma(q^2, \nu)}{d^3p} = 2 \frac{E^*}{p_{\max}^*} \frac{d\sigma(q^2, \nu)}{dx dp_{\perp}^2 d\varphi}, \quad (2)$$

where E^* is the energy of the hadron in the center-of-mass system and p_{\max}^* is the maximum possible center-of-mass momentum.

The experimental apparatus consisted of a 19.5-GeV electron beam incident on a target and a large-aperture spectrometer to detect a large fraction of the forward final-state particles with lab momenta greater than ~ 1 GeV/c. These elements are shown in Fig. 1. The electron beam at the Stanford Linear Accelerator Center (SLAC) contained typically 10^4 e^- per 1.5- μ sec-long pulse. The momentum band was 0.2% at 19.5 GeV/c. The target was 4 cm long and was filled with either hydrogen or deuterium. Only the hydrogen data are reported here. The spectrometer magnet had a field integral of 17 kG m. The unscattered beam and the forward electromagnetic backgrounds passed through the magnet in a field-free region created by a cylindrical supercon-